Lack of Methylated Hopanoids Renders the Cyanobacterium Nostoc punctiforme Sensitive to Osmotic and pH Stress

Lack of methylated hopanoids renders the cyanobacterium *Nostoc punctiforme* sensitive to osmotic and pH stress

Tamsyn J. Garby[1], Emily D. Matys[2], Sarah E. Ongley[1,3], Anya Salih[4], Anthony W.D. Larkum[5] Malcolm R. Walter[1], Roger E. Summons[2#], Brett A. Neilan[1,3#]

[1]Australian Centre for Astrobiology and School of Biotechnology and Biomolecular Sciences, The University of New South Wales, Sydney, NSW 2052, Australia.

[2]Department of Earth, Atmospheric and Planetary Sciences, Massachusetts Institute of Technology, 77 Massachusetts Avenue, Cambridge, MA 02139-4307, USA

[3]School of Environmental and Life Sciences, The University of Newcastle, Callaghan, NSW 2308, Australia.

[4]Confocal Bioimaging Facility, Western Sydney University, NSW 1797, Australia

[5]Plant Functional Biology and Climate Change Cluster, University of Technology Sydney, NSW 2007, Australia

Running title: *Nostoc* mutant devoid of methylated hopanoids

For correspondence: Brett Neilan, brett.neilan@newcastle.edu.au; Roger Summons, rsummons@mit.edu

To investigate the function of 2-methylhopanoids in modern cyanobacteria, the *hpnP* gene coding for the radical SAM methylase protein that acts on the C2 position of hopanoids, was deleted from the filamentous cyanobacterium *Nostoc punctiforme* ATCC 29133S. The resulting Δ*hpnP* mutant lacked all 2-methylhopanoids, but was found to

produce much higher levels of two bacteriohopanepentol isomers compared to the wild type. Growth rates of Δ*hpnP* mutant cultures were not significantly different from those of the wild type under standard growth conditions. Akinete formation was also not impeded by the absence of 2-methylhopanoids. The relative abundances of the different hopanoid structures in akinete-dominated cultures of the wild-type and Δ*hpnP* mutant were similar to those of vegetative cell-dominated cultures. However, the Δ*hpnP* mutant was found to have decreased growth rates under both pH and osmotic stress, confirming a role for 2-methylhopanoids in stress tolerance. Evidence of elevated photosystem II yield and NAD(P)H-dependent oxidoreductase activity in the Δ*hpnP* mutant under stress conditions, compared to the wild type, suggested that the absence of 2-methylhopanoids increases cellular metabolic rates under stress conditions.

Importance: As the first group of organisms to develop oxygenic photosynthesis, Cyanobacteria are central to the evolutionary history of life on Earth and the subsequent oxygenation of the atmosphere. To investigate the origin of cyanobacteria and emergence of oxygenic photosynthesis, geobiologists use biomarkers, the remnants of lipids produced by different organisms that are found in geologic sediments. 2-Methylhopanes have been considered indicative of cyanobacteria in some environmental settings; with the parent lipids 2-methylhopanoids being present in many contemporary cyanobacteria. We have created a *Nostoc punctiforme* Δ*hpnP* mutant strain that does not produce 2-methylhopanoids to assess the influence of 2-methylhopanoids on stress tolerance. Increased metabolic activity in the mutant under stress indicates compensatory alterations of metabolism in the absence of 2-methylhopanoids.

INTRODUCTION

Bacteriohopanepolyols (BHPs) are pentacyclic triterpenoids, hypothesized to be functional analogs of eukaryotic sterols, and widely used as biomarkers for bacteria (1). Hopane hydrocarbons, the diagenetic products of BHPs, are ubiquitous and abundant in ancient sediments (2) and, therefore, potentially useful for evaluating past microbial communities and paleoenvironmental conditions. To this end, it is important to increase our understanding of the sources and functions of specific hopanoid structures. Knowledge about how bacteria adjust their hopanoid production to adapt to different conditions enhances the diagnostic value of fossil lipid assemblages in geologic samples.

Hopanoids occur in a wide range of Gram-negative and Gram-positive bacteria, including those that form symbiotic association with plants (3, 4), yet large gaps still exist in our understanding of the breadth of physiological functions of hopanoids. The localization of hopanoids in membranes has been documented in a variety of different bacteria (5-8). It appears that these lipids influence outer-membrane order and integrity by interacting with lipid A, in a manner analogous to that of cholesterol with sphingolipids in eukaryotes (9-13). There is mounting evidence for the role of hopanoids in protecting cells against a variety of stress conditions, such as increased temperature (5, 14-18), pH and osmotic tension (16, 18, 19), and desiccation (20).

Due to their structural stability, 2-methylhopanoids (2-MeBHPs) in particular are of significant geobiological interest. 2-MeBHPs have been found in significant quantities both in cyanobacterial cultures and cyanobacterial-dominated microbial mats (21, 22), with over twenty strains of cyanobacteria across multiple orders testing positive for 2-MeBHP (reviewed in (23)). Furthermore, episodic spikes in 2-MeBHP abundances in ancient marine sediments and derived oils have been interpreted as possible indicators of modern cyanobacteria thriving during oceanic anoxic events (24, 25). However, a complicating factor is that despite their distribution across all orders of Cyanobacteria, not all nor even a majority

of cyanobacteria have the capability to produce 2-MeBHPs ((23), Garby TJ & Neilan BA, unpublished data).

2-MeBHPs have also long been known to be produced by bacteria other than cyanobacteria (26-30). It was initially thought that these taxa produced only small amounts, which could not account for the abundance of 2-MeBHP in sediments and petroleum. However, it has recently been shown that the anoxygenic phototroph *Rhodopseudomonas palustris* produces 2-MeBHPs in significant amounts (31). Further to this, phylogenetic analysis of HpnP, responsible for the C-2 methylation of BHPs to produce 2-MeBHP, showed a wide distribution in Alphaproteobacteria; this also suggested that it was unlikely that *hpnP* originated in Cyanobacteria (32). This brought into question the validity of using 2-methylhopanes as taxonomic biomarkers for cyanobacteria and led to the proposal that 2-MeBHPs may instead be more generally diagnostic for specific ecological niches (33).

In light of these uncertainties, it is important to learn more about the distribution and physiological role(s) of 2-MeBHPs in cyanobacteria and other bacteria where they are present. Apart from acting as membrane rigidifiers (10), which in turn can influence membrane protein function and transport, the specific functions of 2-MeBHPs in modern cyanobacteria are not well-understood. However, it has been shown that 2-MeBHP are most abundant in the outer membranes of certain cell types, suggesting that C-2 methylation may promote stress resistance (34).

Hopanoids are produced by *N. punctiforme* ATCC 29133 (PCC 73102), a filamentous cyanobacterium of the order Nostocales. This cyanobacteria was originally isolated from a root section taken from a *Macrozamia* sp. cycad (35), and can form symbiotic associations with a number of different plant genera (36). The relationship between *N. punctiforme* and its environment is particularly interesting, as this species can differentiate into a number of cell types in response to external factors (37). Photosynthetic vegetative cells are the usual cell

type under normal conditions, but several specialized cell types can form under stressful conditions. The absence of a nitrogen source, leads to the formation of specialized non-photosynthetic heterocysts capable of fixing atmospheric nitrogen (N_2). Additionally, resting cells called akinetes form in response to nutrient or light limitation. Akinetes are larger and more resistant to stress than vegetative cells, allowing survival until conditions are favorable for growth. Lastly, hormogonia, gliding filaments that are much more motile than vegetative filaments and composed of smaller cells, form in response to a variety of environmental stress signals.

The complex lifecycle of *N. punctiforme* makes it particularly suited for studying the role of hopanoids in stress acclimation. Different cell types contain altered hopanoid profiles, with 2-MeBHP levels being greatest in the outer membranes of akinetes and vegetative cells in N_2-fixing cultures (34). The genome of *N. punctiforme* ATCC 29133 has been sequenced (38), allowing for the identification of genes known to be required for BHP biosynthesis, and particularly that of 2-MeBHP (39). Bacteriohopanetetrol and two isomers of bacteriohopanepentol, bacteriohopane-31,32,33,34,35-pentol (BHpentol-1), and bacteriohopane-30,32,33,34,35-pentol isomer (BHpentol-2), along with their 2-methylated counterparts, have previously been detected in *Nostoc muscorum*, *Nostoc* sp. PCC 6720, and *Nostoc* sp. ATCC 27985 (26, 40, 41). BHpentol-2 bearing a hydroxyl group on C30 has not been reported in taxa other than *Nostoc* sp. and this, together with the R configuration of the hydroxyl at C-34, may be unique to this genus (41).

In this study, we sought to evaluate proposed links between 2-MeBHP and environmental stress (42, 43) and based on geological evidence that suggests some sediments contain anomalously high levels of 2-methylhopanes and implicating them as important for microbial survival (44-46). Specifically we investigated the role of 2-MeBHPs in a modern cyanobacterium, in conferring adaptations to various environmental conditions. To this end,

126 the gene coding for the hopanoid C-2 methylase, *hpnP* (39), was inactivated in *Nostoc*
127 *punctiforme* ATCC 29133S (47). As 2-MeBHPs have previously been linked to a role in both
128 and stress tolerance and akinete formation, it was expected that the absence of 2-
129 methylhopanoid would adversely affect cell survival under a variety of stress conditions and
130 negatively impact the production of akinetes.
131

132 ## MATERIALS AND METHODS

133 **Knockout plasmid construction.** The *hpnP* gene, along with flanking regions of at least 1
134 kb, was amplified from the genome of *Nostoc punctiforme* ATCC 29133S (UCD 153; a
135 spontaneous ATCC 29133 derivate that grows more rapidly and homogenously in liquid,
136 producing slow hormogonia (47)). The primers used for amplification (Table S1) incorporated
137 XhoI restriction sites onto the ends of the amplified product. This PCR product was ligated
138 into the pGEM®-T Easy (Promega) plasmid using the incorporated XhoI restriction sites. A
139 central portion of the cloned *N. punctiforme hpnP* gene, consisting of 1113 bp, was removed
140 by digestion with the restriction enzymes MscI and AleI [New England Biolabs (NEB)].
141 The omega fragment, containing the neomycin-resistance gene (*npt*) and associated *psbA*
142 promoter (PpsbA), of plasmid pSCR9 (48) was isolated by SmaI (NEB) restriction digest. The
143 recovered PpsbA-*npt* cassette from pSCR9 was ligated into the cleaved *hpnP* gene in the
144 pGEM-T plasmid and transformed into competent *Escherichia coli* 5-alpha cells (NEB).
145 Colony PCR was used to screen for inserts containing the PpsbA-*npt* cassette, with the
146 primers hpnP_IF and hpnP_IR (Table S1).
147 The *N. punctiforme hpnP* gene and flanking regions, with the inserted PpsbA-*npt* cassette,
148 was removed from pGEM-T by digestion with the restriction enzyme XhoI (NEB). The
149 plasmid pRL271 (49), a conjugative cyanobacterial suicide vector carrying a counterselective
150 *sacB* gene for selection of double crossovers, was also digested with XhoI, and the resistance

151 cassette inserted. These plasmids were used to transform competent *E. coli* NEB5-alpha
152 (NEB) cells.
153 To confirm sucrose sensitivity conferred by the *Bacillus subtilis* levansucrase *sacB* gene
154 present in the pRL271 plasmid, *E. coli* colonies were grown in LB medium with 5% sucrose
155 and 34 μg/mL of chloramphenicol, and compared to controls grown without sucrose.
156 Purified pRL271 containing the knockout cassette (referred to as HNKO) was used to
157 transform *E. coli* TOP10 competent cells (Invitrogen).
158 **Measurement of *N. punctiforme* culture density.** Chlorophyll a (chl *a*) concentration was
159 used to determine culture density. Duplicate aliquots of 500 μL or 1000 μL were removed,
160 and cells collected by centrifugation. The supernatant was removed, and cells were
161 resuspended in 90% methanol. Cells were lysed using a FastPrep FP120 cell disrupter (MP
162 Biomedicals) instrument at speed 6.0 for 40 s, then left to extract for at least 5 min in the dark.
163 Aliquots were then centrifuged again, and the absorbance of the supernatant measured at 665
164 nm. The concentration of chl *a* was calculated by multiplying the average A_{665} reading by
165 12.7 to obtain μg chl *a* per mL (50).
166 **Triparental conjugation.** The HNKO plasmid was introduced into *Nostoc punctiforme*
167 29133S by triparental conjugation as previously described ((51);
168 http://microbiology.ucdavis.edu/meeks/xpro3.htm), with minor modifications as follows.
169 Briefly, *E. coli* TOP10 harboring HNKO plasmid (donor strain) and *E. coli* JCM113 (helper
170 strain; *E. coli* HB101 carrying both pRK2013 and pRL528 plasmids for mobilization and
171 methylation, respectively) were grown in LB medium containing both chloramphenicol and
172 kanamycin, at 30ºC, until cultures reached an OD_{600} of about 0.7. Cells were washed, and
173 concentrated to OD_{600} 9-10, gently mixed and incubated at room temperature for ~1 h.
174 *Nostoc punctiforme* ATCC 29133S cells from a dense 500 mL culture were harvested by
175 centrifugation and resuspended in 30 mL of fresh Allen & Arnon medium diluted four-fold

(A&A/4). Cultures were disrupted with a Branson digital sonicator in order to fragment filaments to a length of 1-4 cells. Cells were harvested, resuspended in A&A/4 medium containing 5 mM MOPS (pH 7.8) and 2.5 mM NH_4Cl, and placed in low light (~5-10 μE m^2 s^{-1}) to recover for at least 4 h, prior to concentration of the cells to a chl *a* concentration of 100 μg chl *a*/mL.

Sterile conjugation filters (Millipore HATF08250, 0.45 μm, 82 mm) were placed on 1% agar A&A plates containing 5 mM MOPS (pH 7.8), 2.5 mM NH_4Cl and 0.5% LB. Equal amounts (500 μL) of *N. punctiforme* culture and *E. coli* mixture were combined and briefly centrifuged. Supernatant was removed, and the remaining culture was spread onto a conjugation filter. Plates were placed in low light (~5-10 μE m^2 s^{-1}) at 25ºC overnight. All conjugation filters were then transferred to plain A&A 1% agar plates and incubated for a further 4 days.

Growth and selection of Δ*hpnP* mutants. Conjugation filters were transferred to 1% agar A&A plates containing 25 μg/mL neomycin and placed in high light (~25-30 μE m^2 s^{-1}) at 25ºC. *N. punctiforme* colonies that grew on the neomycin selection plates were transferred to 0.5 mL of A&A/4 medium with 25 μg/mL of neomycin and incubated for 2 weeks. At this point, to induce resolution and exclusion of the pRL271 plasmid backbone, the cultures were transferred to 4 mL of A&A/4 medium without neomycin and incubated for two weeks. Cells were recovered by centrifugation, resuspended in 0.5 mL of medium and vortexed. Cells were spread onto 1% agar A&A plates containing 5 mM MOPS, 25 μg/mL neomycin, and 5% (w/v) sucrose to select against cells retaining the pRL271 plasmid backbone, which carries the *sacB* gene. Sucrose resistant colonies were screened by PCR to confirm resolution by double crossover (Fig. S1). The Δ*hpnP* mutant strain was maintained in A&A/4 medium with 25 μg/mL neomycin.

Confirmation of 2-methylhopanoid absence/gene inactivation. Detection and quantification of hopanoids by high-performance liquid chromatography mass spectrometry (LC-MS) was used to confirm the absence of 2-MeBHP production, and assess the production of other BHP compounds in cultures. A fraction of each total lipid extract (TLE) was acetylated with pyridine/acetic anhydride (1:1, v/v) at 70°C for 1 h and left at room temperature overnight. The acetylated TLEs were analyzed by LC-MS. The LC-MS system comprises a 1200 Series HPLC (Agilent Technologies, Santa Clara, CA, USA) equipped with an autosampler and a binary pump linked to a Q-TOF 6520 mass spectrometer (Agilent Technologies) via an atmospheric pressure chemical ionization (APCI) interface (Agilent Technologies) operated in positive ion mode. The analytical procedure was adapted from H. M. Talbot, et al. (52). A Poroshell 120 EC-C18 column (2.1 × 150 mm, 2.7 μm; Agilent Technologies) was chosen to provide fast and high-resolution separations at lower pressures. The APCI parameters were as follows: gas temperature 325°C, vaporizer temperature 350°C, drying gas (N_2) flow 6 l min^{-1}, nebulizer (N_2) flow 30 l min^{-1}, capillary voltage 1200 V, corona needle 4 μA, and fragmentor 150 V.

Hopanoids were identified on the basis of accurate mass measurements of their protonated molecular ions, fragmentation patterns in MS-MS mode, and by comparison (Fig. 1) of relative retention times (53-55). Quantification was accomplished using an external standard, 5β-pregnane-3α,12α-diol-20-one diacetate (PD), chosen because of its structural similarity to hopanoids and because its retention time does not overlap with BHP retention times. However, considerable variability exists in the ionization efficiencies of all hopanoid structures and especially compared to PD (10). Therefore, the relative response factors for BHtetrol and 2-MeBHtetrol were determined using authentic standards and applied to the quantification of all BHP compounds in this study. The relative responses of all BHP, relative to PD, were previously observed to be linear over four orders of magnitude (1). Without

equivalent standards for BHpentol and 2-MeBHpentol, however, our quantification can only be considered approximate for those particular compounds. Since this study focuses on the relative abundance of BHPs, precise quantification for all compounds is not required.

Akinete formation and microscopy. To induce akinete differentiation, cells were transferred to A&A medium without phosphate (56), and placed in very low light (~1-2 μE m^2 s^{-1}). Cells were maintained in these conditions for several weeks. Akinete formation was checked periodically by light microscopy. Sample preparation and electron microscope imaging was performed using an FEI Nova NanoSEM 230 FESEM instrument. Cellular morphology of live N. *punctiforme* cultures was examined by Leica TCS SP5 confocal inverted microscope (Leica Microsystems, Heidelberg). Imaging was performed at excitation by 488 nm line of Argon laser and by 633 nm line of HeNe laser, with emissions at 520-620 nm captured in PMT 1 and emissions at 638-720 nm captured in PMT 2, respectively. Fluorescence emissions from photosynthetic pigments in vegetative and akinete cells (n = 3-4), mainly phycobiliproteins and chlorophyll a (chl *a*), were microspectrally characterised using the λ scan mode of Leica SP5 at excitation by 488 nm by sequentially imaging a series of images from 500 to 750 nm, each acquired at 10-nm emission detection band-width, with 5 nm steps. Spectral data from defined regions of interests (ROIs) inside cells obtained from Leica LAS software was imported into Excel spread-sheet and plotted.

Stress treatments. *Nostoc punctiforme* ATCC 29133S wild-type and Δ*hpnP* mutant cultures were subjected to a variety of stress conditions. Cells were grown in A&A/4 medium (without neomycin) at 25ºC on a shaking platform under cool white fluorescent lights (~20 μE m^2 s^{-1}) until they reached mid-log phase, then transferred to the stress treatments. Two different experimental designs for growing cells under stress conditions were used, covering a range of temperatures, pH levels, and salt concentrations. The standard growth conditions used for control cultures in all experiments were: 25ºC, 1.1 mM NaCl, and pH 7.8.

First, cultures were subjected to heat stress (34ºC), osmotic stress (100 mM NaCl) and pH stress (6.0 and 9.5). The media for control, salt and heat stress treatments media were buffered to pH 7.8 with 10 mM HEPES. The medium for the pH 9.5 treatment was buffered with 10 mM sodium carbonate – sodium bicarbonate, and the medium for the pH 6.0 treatment was buffered with 10 mM MES. Three biological replicates were maintained for each treatment, under continuous light on a shaking platform. At the beginning of the trial, 130 mL of each type of medium was inoculated with cells at an initial density of approximately 0.1 µg chl *a* per mL. Growth was measured over the course of several weeks by chl *a* extraction as described above. The maximum quantum yield of photosystem II (PSII) (F_v/F_m) of each culture was also measured at various times over the course of the trial as described below.

Second, a range of pH levels and NaCl concentrations were evaluated concurrently. The range of pH levels was from 4.8 to 10.0, and the range of NaCl concentrations was 100-180 mM. Four biological replicates were maintained for each treatment, under continuous light on a shaking platform. Cultures were grown in a 24-well plate, where 2 mL of medium in each well was inoculated with cells at an initial density of approximately 0.6 µg chl *a* per mL. Media for cultures grown at pH levels from 6.0-6.5 were buffered with 10 mM MES, media for cultures grown at pH levels from 6.8-8.2 were buffered with 10 mM HEPES, and media for cultures grown at pH levels from 8.5-9.0 were buffered with 10 mM Tris. Growth was measured over the course of several weeks by chl *a*, and MTT [3-(4,5-dimethylthiazol-2-yl)-2,5-diphenyltetrazolium bromide] assays were performed as described below.

Cells were also subjected to stress caused by freezing. Cultures were concentrated by centrifugation to approximately 12 µg chl *a* per mL, then 1 mL aliquots were vortexed to homogenize cultures. These 1 mL aliquots were placed in a freezer at -20ºC, in two sets of biological triplicates. One set was thawed and refrozen twice over one week, and the second set thawed and refrozen three times over two weeks. After final removal from the freezer,

thawed cells were used to inoculate 50 mL of A&A/4 medium, and left to recover under control conditions. Growth was measured over the course of several weeks by chl *a* extraction.

PAM fluorometry. A portable Pulse Amplitude Modulation (PAM) fluorometer 2500 (Walz) was used to measure F_v/F_m. F_v/F_m is an indicator of PSII efficiency, which can in turn be used as an indicator of overall cell health. Aliquots of 1 mL were removed from cultures and dark adapted for a minimum of 10 min, then placed under a weak red measuring light. Cells were exposed to a strong red saturation pulse of 100 ms in duration to measure the maximum (dark adapted) yield of PSII (F_v/F_m). Slow kinetics curves were determined for cells from each treatment by applying red actinic light for 250 s, with a saturation pulse every 20 s.

MTT assays. The MTT assay was used to assess cell proliferation based on the NAD(P)H-dependent oxidoreductase enzyme activity of cells. Cell densities were standardized to the lowest density present according to chl *a* measurements. Cells were resuspended in 100 µL of medium in a 96-well plate, using four biological replicates for each treatment. A 20 µL solution of 5 mg/mL MTT (Thiazolyl Blue Tetrazolium Blue, Sigma Aldrich) was added, and samples were incubated at 37ºC for 2 h. Plates were centrifuged, medium was removed from the wells, and 200 µL of acidic isopropanol (0.04 M HCl) was added to each well and mixed. Absorbance was measured at 570 nm, with higher absorbance readings corresponding to a higher level of metabolic function.

Statistical analysis. Slopes of the exponential phase of growth curves for cultures treated by heat stress, pH 6.0, pH 9.5, 100 mM NaCl and freezing were calculated in Prism v. 6.0, and one-way ANOVA tests were performed to compare slopes.

For cell densities of cultures grown in a range of pH levels and NaCl concentrations, values were adjusted to account for differences between cultures of wild-type and Δ*hpnP*

mutant cells under control conditions. Assuming exponential growth, growth rates of treatment cultures were normalized to average control culture growth rates at each time point following the formula:

$\text{density}A_x \times (\text{density}B_{\text{control\_average}}/\text{density}A_{\text{control\_average}})$,

where A is the slower-growing culture under optimal conditions and B is the faster-growing culture under optimal conditions. Densities of cultures in each treatment at each time point were compared separately by one-way ANOVA tests.

For MTT assays, values were adjusted to account for differences between cultures of wild-type and Δ*hpnP* mutant cells under control conditions. Assuming a linear relationship between NAD(P)H-dependent enzyme activity and the A_{570} values observed, values for treatment cultures were normalized to average control culture values at each time point following the formula:

$\text{density}A_x + (\text{density}B_{\text{control\_average}} - \text{density}A_{\text{control\_average}})$,

A and B are defined as above. Absorbance readings of assays from each treatment at each time point were compared separately by one-way ANOVA tests.

RESULTS

Confirmation of gene inactivation. PCR amplification and sequencing of *hpnP* and flanking loci showed the successful substitution of the central region of the *hpnP* gene with the neomycin-resistance cassette of pSCR9. Additionally, PCRs performed with primers internal to the deleted section of the *hpnP* gene failed to amplify any product from the genomes of mutated cells.

Hopanoid profiles. Hopanoid analyses of *N. punctiforme* wild-type and Δ*hpnP* mutant vegetative and akinete cells revealed six BHP compounds (Fig. 1). Bacteriohopanetetrol (BHtetrol) and methylated counterpart, 2-methylbacteriohopanetetrol (2-MeBHtetrol) were

present in wild-type vegetative and akinete cell types. BHtetrol was present while 2-MeBHtetrol was absent in all Δ*hpnP* mutants. Bacteriohopanepentol (BHpentol) was identified, as well as a putative isomer, denoted BHpentol-1 and BHpentol-2. 2-Methylbacteriohopanepentol (2-MeBHpentol) was also identified, as well as a putative isomer, denoted 2-MeBHpentol-1 and 2-MeBHpentol-2. 2-MeBHpentol-1 and -2 were the most abundant compounds in wild-type vegetative and akinete cell types and were absent in all Δ*hpnP* mutant cell types. BHpentol-2 and 2-MeBHpentol-2 were not detected by GC-MS, and required LC-MS techniques for identification.

A clear change was observed in the diversity and abundance of BHPs produced by wild-type *N. punctiforme* and Δ*hpnP* mutant strain cell types (Fig. 2). LC-MS analysis using authentic standards enabled the robust quantification of BHP compounds (Fig. 1). Total BHP is greater in vegetative cells as compared to the akinete cell type in both wild type and Δ*hpnP* mutants. Total BHP is greater in wild type cells (vegetative and akinete) as compared to Δ*hpnP* mutant cells. While Δ*hpnP* vegetative and akinete cell mutants do not produce 2-MeBHP, the abundance of BHpentol-1, BHpentol-2, and BHtetrol increase, possibly compensating for the lack of 2-MeBHPs produced. Both wild type vegetative and akinete cells contained an order of magnitude more methylated BHPs as compared to desmethyl BHPs. Total BHP is ~75% greater in wild-type vegetative cells than wild-type akinetes. However, total BHP is only ~35% greater in Δ*hpnP* mutant vegetative cells compared to Δ*hpnP* akinetes. Wild-type cells still produce ~30% more BHPs than Δ*hpnP* mutants due to their high abundance of non-methylated compounds.

Akinete formation. Cultures were induced to form akinetes to determine if the lack of 2-methylhopanoids impeded this process. Akinete formation was not affected by the lack of 2-methylhopanoids, with the Δ*hpnP* mutant culture forming filaments of akinetes as readily as the wild-type culture (Fig. 3, 4). Confocal imaging revealed no differences in the cell shape,

the size or fluorescence emission intensity between wild-type and Δ*hpnP* mutant *N. punctiforme*. Akinete dominated cultures had more rounded cells and many were larger in size that the vegetative cells (Fig. 4A, B). It was also observed that hormogonia filaments formed alongside the akinetes in the wild-type culture, whereas in the Δ*hpnP* mutant culture hormogonia filaments were rare.

Fluorescence emissions were highest in the orange and the red wavebands due to phycobilins and chlorophyll (Fig. 4). Microspectral confocal imaging identified prominent in vivo emission peaks due to the photosynthetic pigments typical to *Nostoc* spp. These were due to phycoerythrin (PE), with emission maximum (em_{max}) at 575 nm, phycocyanin (PC) with em_{max} = 625-645 nm and allophycocyanin (ALP), em_{max} = 660-665nm, with shoulders at 675-690 (chlorophyll a photosystem II, chl PSII) and far-red emissions at 710 nm (chl photosystem I, PSI) (Fig. 4C).

There was a distinct increase in the PE emissions relative to other peaks in akinetes, which was most prominent in Δ*hpnP* mutant cells, and lowest in the Δ*hpnP* mutant vegetative cells (Fig. 4C). Akinetes were also observed to have reduced levels of ALP, as well as of chl *a* PSII and PSI emissions, compared to the vegetative cells (Fig. 4C). The differences were especially prominent in mutant Δ*hpnP* cells. Since 2-methylhopanoids are not known to be functionally linked to oxygenic photosynthesis, the cause of these differences in pigment expression in mutant Δ*hpnP* cells is presently unknown.

Mutant response to temperature stress. *N. punctiforme* ATCC 29133S wild-type and Δ*hpnP* cultures were subjected to stress caused by elevated temperature and freezing/thawing. Based on chl *a* levels, cultures of *N. punctiforme* Δ*hpnP* mutant cells grown at 34ºC did not grow significantly more slowly than wild-type cultures (Fig. 5). Cultures of *N. punctiforme* Δ*hpnP* mutant cells frozen and thawed over a period of 2 weeks and then used to inoculate media and incubated at 25ºC failed to grow in two out of three replicates, as opposed to

cultures from similarly treated *N. punctiforme* wild-type cultures, where all three replicates recovered and resumed growth. F_v/F_m was measured for control cultures and heat-treated cultures over the course of five weeks to obtain a measurement of photosynthetic efficiency as an indication of cell health (Fig. S3A). F_v/F_m values for both heat-stressed cultures were consistently higher than F_v/F_m values for both control condition cultures. There was no significant difference in F_v/F_m values between *N. punctiforme* wild-type and Δ*hpnP* cells in either control or heat-stress conditions.

Mutant response to variable pH. *N. punctiforme* ATCC 29133 wild-type and Δ*hpnP* cultures were subjected to different pH values in two separate experimental designs. At pH 9.5 the growth rate of both the wild-type and Δ*hpnP* mutant did not significantly vary from the control condition (Fig. 5). Growth rates for both treated cultures began to decline after 10 days, however the wild-type did not vary considerably from the control over the course of the experiment, indicating a faster stress adaptation. Culture density of the Δ*hpnP* mutant was significantly lower than that of the wild-type after 23 days, supporting a faster adaptation of the wild-type to the high pH stress condition.

When a range of pH values were tested over several weeks, there was a significant difference in culture density between the wild-type and Δ*hpnP* strains grown in pH levels of 6.0, 6.2, 6.5, 6.8 and 7.0 after 5 weeks (Fig. 6A). Cultures grown at higher pH values (7.8-9.0) did not survive the duration of the experiment.

F_v/F_m was measured for control cultures and cultures grown at pH 6.0 and pH 9.5 over the course of 5 weeks (Fig. S3B). F_v/F_m values for cultures grown at pH 6.0 were no different from those grown in control conditions, and there was also no difference between wild-type and Δ*hpnP* mutant cultures. The F_v/F_m values for cultures grown at pH 9.5 varied over time, with a drop in F_v/F_m around days 13-30 corresponding to a decreased growth rate over this

399 period. F_v/F_m values of the Δ*hpnP* mutant culture remained higher than those of the wild-type
400 culture over this period.
401 An MTT assay was performed on *N. punctiforme* wild-type and Δ*hpnP* cells that had been
402 growing at pH levels from 6.0 to 7.8 for 4 weeks. Values were significantly higher for the
403 mutant cells across all pH values from 6.0 to 7.0 (Fig. S4).
404 **Δ*hpnP* mutant response to osmotic stress.** *N. punctiforme* ATCC 29133S wild-type and
405 Δ*hpnP* cultures were subjected to a variety of different concentrations of NaCl in two
406 different experimental designs. There was a significant difference in culture density between
407 the wild-type and Δ*hpnP* strains grown in concentrations of NaCl of 100 mM, 120 mM, 140
408 mM, 160 mM and 180 mM for 5 weeks (Fig. 6B).
409 F_v/F_m was measured for control cultures and cultures grown at 100 mM NaCl over the
410 course of 5 weeks. F_v/F_m values of both NaCl-treated cultures were consistently higher than
411 those of the control cultures, and F_v/F_m values of the Δ*hpnP* mutant cells grown in 100 mM
412 NaCl were significantly higher than those of the wild-type cells grown in the same conditions
413 (Fig. S3C).
414 An MTT assay was performed on *N. punctiforme* wild-type and Δ*hpnP* cells that had been
415 growing at concentrations of NaCl from 1.1 mM to 180 mM for 4 weeks. Absorbance values
416 were significantly higher for the mutant cells across all NaCl concentrations from 120 mM to
417 180 mM (Fig. S4).
418

419 ## DISCUSSION

420 **Hopanoid production in the Δ*hpnP* mutant.** It has previously been shown that in *Nostoc* sp.
421 PCC 6720, 2-MeBHPs are produced in far greater abundance than their non-methylated
422 analogs (41). The results presented here were consistent with this. In the Δ*hpnP* mutant cells,
423 the abundance of non-methylated pentols increased by 1-2 orders of magnitude, resulting in

424 the combined level of hopanoids being similar for the wild-type and Δ*hpnP* mutant cells. The
425 increased production of BHpentol-1 and BHpentol-2 in the Δ*hpnP* mutant is likely a response
426 to the inability to produce methylated hopanoids.
427 The lack of 2-MeBHPs in the Δ*hpnP* cultures did not impede the cells' ability to form
428 akinetes, which indicates these lipids are not essential for the formation of resting cells under
429 normal conditions. However, as akinetes can survive extreme conditions (57, 58) that were
430 not tested here, it may be that 2-MeBHP is more important for akinete survival against
431 external stresses than for their formation, however this is beyond the scope of the current
432 study.
433 The present examination of akinete-dominated cultures of wild-type and Δ*hpnP* mutant
434 cells followed the results of Doughty et al. (34), who found a large increase in the amount of
435 2-methylhopanoids, especially 2-MeBHtetrol, in akinete outer membranes of *N. punctiforme*
436 compared to other cell membrane types. In the present study, no change in the relative
437 abundances of 2-MeBHPs/BHPs was detected between vegetative cell and akinete-dominated
438 cultures (Fig. 2). In comparing the quantitative aspects of the data, however, it is important to
439 note that Doughty et al. (34) used GC-MS and conducted semiquantitative analyses of the
440 lipid contents of isolated membrane fractions as opposed to the data reported here which is
441 based on LC-MS and is for whole cells. More significantly, the bulk of BHP in this strain of
442 *Nostoc punctiforme* is in the form of the two BHpentols and their methylated counterparts.
443 These have longer retention times than BHtetrol and are likely less thermally stable. Thus, it
444 is probable that a significant amount decomposed during the GC-MS analyses reported by
445 Doughty et al. (2009), as evidenced by the presence of a single BHpentol GC peak and
446 thereby rendering the quantification less reliable in that earlier study. In this work we also
447 improved the quantitative rigor by employing an internal standard PD and authentic standards

448 of BHtetrol and 2-MeBHtetrol (10) to determine the relative APCI response factors for these
449 compounds which were slightly but measurably different.

450 **Response of the Δ*hpnP* mutant to physiological stress.** Cyanobacteria flourish in a
451 variety of environments where factors such as temperature, pH and salt concentrations are
452 considered outside the optimal range for most bacteria. Cyanobacterial cells consequently
453 have developed adaptations in order to protect themselves against these conditions. Culture
454 conditions used here simulate those found in many extreme environments where
455 cyanobacteria thrive, such as desert soil crusts, hot springs, hypersaline pools, and Antarctic
456 melt water pools.

457 The Δ*hpnP* mutant was less resistant to pH and osmotic stress than the wild type. The role
458 of 2-MeBHPs in stress tolerance against pH and osmotic stress is consistent with the findings
459 of Kulkarni et al. (18) in *Rhodopseudomonas*, except that they found a regulatory effect on
460 *hpnP* only in the presence of non-ionic osmolytes.

461 The influence of hopanoids on the tolerance of temperature stresses has been investigated
462 in *Rhodopseudomonas* (18) and *Nostoc punctiforme* (42). Our findings were in agreement
463 with these studies as there was no significant difference between the growth rates or the PSII
464 efficiency of wildtype and Δ*hpnP* strains under elevated temperature. Studies of microbial
465 mats from Antarctic melt water ponds (59) and Arctic soils (60) suggest that hopanoids may
466 play a role in cryoprotection. We investigated this by subjecting the wildtype and Δ*hpnP*
467 mutant to freezing in the absence of an exogenous cryoprotectant. Survival of wildtype
468 cultures was greater than the Δ*hpnP* mutant, indicating that the absence of 2-MeBHPs
469 decreases the tolerance of cells to freezing; however, this should be investigated more
470 thoroughly at various temperatures and time scales.

471 F_v/F_m values reflect the efficiency of PSII, while MTT absorbance readings reflect the
472 activity of NAD(P)H-dependent cellular oxidoreductases. Under control culture conditions,

473 no difference in growth rate or F_v/F_m values was observed between wild-type and Δ*hpnP*
474 mutant cultures. However, when differences (albeit not statistically significant) in growth
475 rates between the two strains became apparent, these were reflected in differing F_v/F_m values
476 and oxidoreductase activity (MTT assays). F_v/F_m for the slower-growing Δ*hpnP* mutant
477 cultures were higher than those for the wild-type cultures. From the MTT assays, absorbance
478 readings were higher for Δ*hpnP* mutant cells under salt and pH stress than for wild-type cells
479 under the same stress. Taken together, the fact that values were consistently higher for Δ*hpnP*
480 mutant cells than for wild-type cells under stress indicates an increased metabolic rate in the
481 mutant strain, possibly as a compensatory stress response to reduced protection by hopanoids.
482 This likely resulted in an increase of other protective strategies, that require energy to
483 maintain homeostasis rather than for growth. In addition, our finding of differences in the
484 emission signals from the photosynthetic pigments in Δ*hpnP* mutant cultures, with substantial
485 increases of phycoerythrin emissions in mutant akinete-dominated cultures, compared to wild-
486 type akinetes (and both vegetative cultures), may similarly be related to compensatory
487 strategies in cells lacking hopanoids.

488 The presence of 2-MeBHPs does not appear to be necessary for *N. punctiforme* cell
489 function under standard laboratory growth conditions. 2-MeBHPs do, however, appear to aid
490 cyanobacterial cells to resist a variety of stress conditions including pH and osmotic stress.
491 Similar observations have been made in hopanoid mutants of *Burkholderia cenocepacia* (61)
492 and *Rhodopseudomonas palustris* (19) that was attributed to a decrease in outer membrane
493 integrity. While Doughty et al (2009) found that 2-MeBHPs were highest in akinetes, they are
494 also present in vegetative cells being localised between the cells of the filament (6). We
495 observed that cells within Δ*hpnP* filaments were not as closely packed (Fig. 3), with this
496 decreased filament integrity at the cell-cell junction potentially increasing the sensitivity of
497 the Δ*hpnP* mutant to stressors. Contrary to our original hypothesis, 2-MeBHPs were not

necessary for *N. punctiforme* cells to form akinetes under phosphate-limitation and low-light conditions. Akinete outer membrane integrity is not impaired by the absence of 2-MeHPNs, however the total absence of hopanoids (Δ*shc* mutant) results in a substantial decrease of akinete resilience, as determined by lysozyme treatment (42). Although the resistance of akinetes lacking 2-MeBHPs to other stresses is yet to be tested.

Conclusions. Given the importance of 2-MeBHPs in the adaptation to environmental stressors such as pH, and their dominance in the resting cell-type, the presence of 2-MeBHPs in geological sediment samples are indicative of periods of climate disturbances necessitating adaptation or senescence. As *hpnP* diversity was quite high in desert environments sampled, testing the *N. punctiforme* Δ*hpnP* mutant's resistance to UV radiation and desiccation under conditions similar to those experienced by desert biological soil crust communities would be quite relevant (62). The preliminary evidence for a role for 2-MeBHPs in *N. punctiforme* in protection against freezing/thawing stress found here should be followed up with trials over different temperatures, cycles and durations. Unfortunately, we cannot distinguish between the effects of lower amounts of BHPs vs the loss of 2-MeBHP, however complementary experiments utilizing a hopanoid-null mutant may further clarify their role. Overall, the *Nostoc punctiforme* Δ*hpnP* mutant created here provides a useful tool for investigating the role of 2-methylhopanoids in cyanobacteria.

ACKNOWLEDGEMENTS

The authors would like to acknowledge the services of the University of New South Wales Electron Microscopy Unit and the Ramaciotti Centre for Genomics.

Work undertaken at UNSW was supported by The Australian Research Council. Work undertaken at MIT was supported by an award (NNA13AA90A) from the NASA Astrobiology Institute. We thank C.H. Wu and D.K. Newman for the provision of authentic

standards of BHtetrol and 2-MeBHtetrol, and J.C. Meeks for provision of the *N. punctiforme* 29133S and *E. coli* JCM113 strains.

Supplementary information is available on the Internet.

FIGURE LEGENDS

Figure 1. Abundance of hopanoids as analyzed by LC-MS. The lipid content of wild-type (WT) and ΔhpnP cultures dominated by late exponential phase vegetative cells or akinetes was characterized. Hopanoids (mg BHPs/g cellular material) detected in each sample is given below the cellular type. Quantification was completed using authentic BHtetrol and 2-MeBHtetrol standards. Values were averaged from 2 LC-MS runs (June 4, 2014 and June 16, 2015). Error bars represent 1 standard deviation.

Figure 2. Typical LC chromatograms showing the elution patterns of acetylated hopanoids from wild-type (WT) and Δ*hpnP* cultures dominated by vegetative cells or akinetes. BHpentol-1 is tentatively identified as bacteriohopane-31,32,33,34,35-pentol based on its elution position relative to that compound in other samples. BHpentol-2 is assigned as bacteriohopane-30,32,33,34,35-pentol previously identified by Zhao et al. (1996). The 2-methyl analogs of these compounds are identified, similarly, by their relative retention times. BHT is bacteriohopane-32,33,34,35-tetrol and 2-MeBHT is its 2-methyl analog.

Figure 3. Differential interference contrast micrographs (A-D) and SEM images (E, F) of cultures of wild-type *N. punctiforme* (A, C, E) and the Δ*hpnP* mutant (B, D, F), under control conditions (A, B) showing vegetative cell filaments with heterocysts (Het), and sixteen weeks

after transfer to phosphate-free medium and low light conditions (C-F), showing formation of akinetes (Ak) amongst vegetative filaments (Veg).

Figure 4. Confocal imaging of fluorescence emissions of *N. punctiforme* with emissions from PMT1 (520-620 nm) and PMT 2 (638-700 nm) combined - (A) akinete-dominated culture of wild-type; (B) the Δ*hpnP* mutant stages; and (C) confocal microspectral detection of photosynthetic pigments in wild-type vegetative stages (red solid line) and akinete stages (red dashed line); of the Δ*hpnP* mutant vegetative (green solid line) and mutant akinete (dashed green line) stages. The spectral emission peak at 575 nm is for phycoerythrin (PE), at 645 nm - phycocyanin (PC), at 660 nm - allophycocyanin (APC), the shoulder at 680 nm - chlorophyll a photosystem II (Chl PSII) and at 710 nm - Chl photosystem I (Chl PSI).

Figure 5. Growth curves of *N. punctiforme* wild-type and Δ*hpnP* cultures grown under control conditions (pH 7.8, 25ºC), heat stress (34ºC), and high pH stress (pH 9.5), based on chl *a* concentration. Error bars represent SE from the mean of three independent cultures.

Figure 6. Density of *N. punctiforme* wild-type and Δ*hpnP* cultures grown at a range of pH levels from 7.8 to 6.0 (A) or a range of NaCl concentrations from 1.1 mM to 180 mM (B) after five weeks. Measurements are relative to the density of cultures grown in control conditions (pH 7.8, 1.1 mM NaCl), based on chl *a* concentration. Error bars represent SE from the mean of three to four independent cultures. Culture density at weeks 3 and 4 are shown in Fig. S2.

REFERENCES

1. Sáenz JP, Waterbury JB, Eglinton TI, Summons RE. 2012. Hopanoids in marine cyanobacteria: probing their phylogenetic distribution and biological role. Geobiology. 10:311-319. 10.1111/j.1472-4669.2012.00318.x
2. Ourisson G, Albrecht P. 1992. Hopanoids. 1. Geohopanoids: The most abundant natural products on Earth? Accounts of Chemical Research. 25:398-402. 10.1021/ar00021a003
3. Kannenberg EL, Perzl M, Müller P, Härtner T, Poralla K. 1996. Hopanoid lipids in *Bradyrhizobium* and other plant-associated bacteria and cloning of the *Bradyrhizobium japonicum* squalene-hopene cyclase gene. Plant Soil. 186:107-112. 10.1007/BF00035063
4. Kannenberg EL, Poralla K. 1999. Hopanoid biosynthesis and function in bacteria. Naturwissenschaften. 86:168-176. 10.1007/s001140050592
5. Doughty DM, Coleman ML, Hunter RC, Sessions AL, Summons RE, Newman DK. 2011. The RND-family transporter, HpnN, is required for hopanoid localization to the outer membrane of *Rhodopseudomonas palustris* TIE-1. Proceedings of the National Academy of Sciences. 108:E1045-1051. 10.1073/pnas.1104209108
6. Doughty DM, Dieterle M, Sessions AL, Fischer WW, Newman DK. 2014. Probing the subcellular localization of hopanoid lipids in bacteria using NanoSIMS. PLoS ONE. 9:e84455. 10.1371/journal.pone.0084455
7. Jürgens UJ, Simonin P, Rohmer M. 1992. Localization and distribution of hopanoids in membrane systems of the cyanobacterium *Synechocystis* PCC 6714. FEMS Microbiology Letters. 71:285-288. 10.1016/0378-1097(92)90723-2
8. Simonin P, Jürgens UJ, Rohmer M. 1996. Bacterial triterpenoids of the hopane series from the prochlorophyte *Prochlorothrix hollandica* and their intracellular localization. European Journal of Biochemistry. 241:865-871. 10.1111/j.1432-1033.1996.00865.x
9. Poralla K, Kannenberg E, Blume A. 1980. A glycolipid containing hopane isolated from the acidophilic, thermophilic *Bacillus acidocaldarius*, has a cholesterol-like function in membranes. FEBS Letters. 113:107-110. 10.1016/0014-5793(80)80506-0
10. Wu C-H, Bialecka-Fornal M, Newman DK. 2015. Methylation at the C-2 position of hopanoids increases rigidity in native bacterial membranes. eLife. 4. 10.7554/eLife.05663
11. Silipo A, Vitiello G, Gully D, Sturiale L, Chaintreuil C, Fardoux J, Gargani D, Lee H-I, Kulkarni G, Busset N, Marchetti R, Palmigiano A, Moll H, Engel R, Lanzetta R, Paduano L, Parrilli M, Chang W-S, Holst O, Newman DK, Garozzo D, D'Errico G, Giraud E, Molinaro A. 2014. Covalently linked hopanoid-lipid A improves outer-membrane resistance of a *Bradyrhizobium* symbiont of legumes. Nature Communications. 5:5106. 10.1038/ncomms6106
12. Komaniecka I, Choma A, Mazur A, Duda KA, Lindner B, Schwudke D, Holst O. 2014. Occurrence of an unusual hopanoid-containing lipid A among lipopolysaccharides from *Bradyrhizobium* species. J Biol Chem. 289:35644-35655. 10.1074/jbc.M114.614529
13. Sáenz JP, Grosser D, Bradley AS, Lagny TJ, Lavrynenko O, Broda M, Simons K. 2015. Hopanoids as functional analogues of cholesterol in bacterial membranes. Proceedings of the National Academy of Sciences. 112:11971-11976. 10.1073/pnas.1515607112
14. Caron B, Mark AE, Poger D. 2014. Some like it hot: the effect of sterols and hopanoids on lipid ordering at high temperature. The journal of physical chemistry letters. 5:3953-3957. 10.1021/jz5020778
15. Joyeux C, Fouchard S, Llopiz P, Neunlist S. 2004. Influence of the temperature and the growth phase on the hopanoids and fatty acids content of *Frateuria aurantia* (DSMZ 6220). FEMS Microbiol Ecol. 47:371-379. 10.1016/S0168-6496(03)00302-7
16. Poralla K, Htrtner T, Kannenberg E. 1984. Effect of temperature and pH on the hopanoid content of *Bacillus acidocaldarius*. FEMS Microbiology Letters. 23:253-256. 10.1111/j.1574-6968.1984.tb01073.x

17. Schmidt A, Bringer-Meyer S, Poralla K, Sahm H. 1986. Effect of alcohols and temperature on the hopanoid content of *Zymomonas mobilis*. Applied Microbiology and Biotechnology. 25:32-36. 10.1007/BF00252509
18. Kulkarni G, Wu C-H, Newman DK. 2013. The general stress response factor EcfG regulates expression of the C-2 hopanoid methylase HpnP in *Rhodopseudomonas palustris* TIE-1. Journal of Bacteriology. 195:2490-2498. 10.1128/JB.00186-13
19. Welander PV, Hunter RC, Zhang L, Sessions AL, Summons RE, Newman DK. 2009. Hopanoids play a role in membrane integrity and pH homeostasis in *Rhodopseudomonas palustris* TIE-1. Journal of Bacteriology. 191:6145-6156. 10.1128/JB.00460-09
20. Poralla K, Muth G, Härtner T. 2000. Hopanoids are formed during transition from substrate to aerial hyphae in *Streptomyces coelicolor* A3(2). FEMS Microbiology Letters. 189:93-95. 10.1111/j.1574-6968.2000.tb09212.x
21. Jahnke LL, Embaye T, Hope J, Turk KA, M VZ, Des Marais DJ, Summons RE. 2004. Lipid biomarker and carbon isotopic signatures for stromatolite-forming, microbial mat communities and *Phormidium* cultures from Yellowstone National Park. Geobiology. 2:31-47. 10.1111/j.1472-4677.2004.00021.x
22. Summons RE, Jahnke LL, Hope JM, Logan GA. 1999. 2-Methylhopanoids as biomarkers for cyanobacterial oxygenic photosynthesis. Nature. 400:554-557. 10.1038/23005
23. Talbot HM, Summons RE, Jahnke LL, Cockell CS, Rohmer M, Farrimond P. 2008. Cyanobacterial bacteriohopanepolyol signatures from cultures and natural environmental settings. Organic Geochemistry. 39:232-263. 10.1016/j.orggeochem.2007.08.006
24. Knoll AH, Summons RE, Waldbauer JR, Zumberge J. 2007. The geological succession of primary producers in the oceans, p 133-163. *In* Falkowski PG, Knoll AH (ed), Evolution of primary producers in the sea. Elsevier, Boston.
25. Kuypers MMM, van Breugel Y, Schouten S, Erba E, Sinninghe Damsté JS. 2004. N2-fixing cyanobacteria supplied nutrient N for Cretaceous oceanic anoxic events. Geology. 32:853. 10.1130/G20458.1
26. Bisseret P, Zundel M, Rohmer M. 1985. Prokaryotic triterpenoids 2. 2β-methylhopanoids from Methylobacterium organophilum and *Nostoc muscosum*, a new series of prokaryotic triterpenoids. European Journal of Biochemistry. 150:29-34. 10.1111/j.1432-1033.1985.tb08982.x
27. Bravo JM, Perzl M, Härtner T, Kannenberg EL, Rohmer M. 2001. Novel methylated triterpenoids of the gammacerane series from the nitrogen-fixing bacterium *Bradyrhizobium japonicum* USDA 110. European Journal of Biochemistry. 268:1323-1331. 10.1046/j.1432-1327.2001.01998.x
28. Renoux JM, Rohmer M. 1985. Prokaryotic triterpenoids. New bacteriohopanetetrol cyclitol ethers from the methylotrophic bacterium *Methylobacterium organophilum.* European Journal of Biochemistry. 151:405-410. 10.1111/j.1432-1033.1985.tb09116.x
29. Stampf P, Herrmann D, Bisseret P, Rohmer M. 1991. 2α-Methylhopanoids: First recognition in the bacterium *Methylobacterium organophilum* and obtention via sulphur induced isomerization of 2β-methylhopanoid. An account for their presence in sediments. Tetrahedron. 47:7081-7990. 10.1016/s0040-4020(01)96162-9
30. Vilcheze C, Llopiz P, Neunlist S, Poralla K, Rohmer M. 1994. Prokaryotic triterpenoids: new hopanoids from the nitrogen-fixing bacteria *Azotobacter vinelandii*, *Beijerinckia indica* and *Beijerinckia mobilis* Microbiology. 140:2749-2753. 10.1099/00221287-140-10-2749
31. Rashby SE, Sessions AL, Summons RE, Newman DK. 2007. Biosynthesis of 2-methylbacteriohopanepolyols by an anoxygenic phototroph. Proceedings of the National Academy of Sciences. 104:15099-15104. 10.1073/pnas.0704912104

669 32. Ricci JN, Michel AJ, Newman DK. 2015. Phylogenetic analysis of HpnP reveals the
670 origin of 2-methylhopanoid production in Alphaproteobacteria. Geobiology. 13:267-277.
671 10.1111/gbi.12129
672 33. Ricci JN, Coleman ML, Welander PV, Sessions AL, Summons RE, Spear JR, Newman
673 DK. 2014. Diverse capacity for 2-methylhopanoid production correlates with a specific
674 ecological niche. ISME J. 8:675-684. 10.1038/ismej.2013.191
675 34. Doughty DM, Hunter RC, Summons RE, Newman DK. 2009. 2-Methylhopanoids are
676 maximally produced in akinetes of *Nostoc punctiforme*: geobiological implications.
677 Geobiology. 7:524-532. 10.1111/j.1472-4669.2009.00217.x
678 35. Rippka R, Deruelles J, Waterbury JB, Herdman M, Stanier RY. 1979. Generic
679 assignments, strain histories and properties of pure cultures of cyanobacteria.
680 Microbiology. 111:1-61. doi:10.1099/00221287-111-1-1
681 36. Meeks JC. 1998. Symbiosis between nitrogen-fixing cyanobacteria and plants. Bioscience.
682 48:266-276. 10.2307/1313353
683 37. Meeks JC, Campbell EL, Summers ML, Wong FC. 2002. Cellular differentiation in the
684 cyanobacterium *Nostoc punctiforme.* Archives of Microbiology. 178:395-403.
685 10.1007/s00203-002-0476-5
686 38. Meeks JC, Elhai J, Thiel T, Potts M, Larimer F, Lamerdin J, Predki P, Atlas R. 2001. An
687 overview of the genome of *Nostoc punctiforme*, a multicellular, symbiotic
688 cyanobacterium. Photosynthesis Research. 70:85-106. 10.1023/A:1013840025518
689 39. Welander PV, Coleman ML, Sessions AL, Summons RE, Newman DK. 2010.
690 Identification of a methylase required for 2-methylhopanoid production and implications
691 for the interpretation of sedimentary hopanes. Proceedings of the National Academy of
692 Sciences. 107:8537-8542. 10.1073/pnas.0912949107
693 40. Rohmer M, Bouviernave P, Ourisson G. 1984. Distribution of hopanoid triterpenes in
694 prokaryotes. J Gen Microbiol. 130:1137-1150. 10.1099/00221287-130-5-1137
695 41. Zhao N, Berova N, Nakanishi K, Rohmer M, Mougenot P, Jürgens UJ. 1996. Structures of
696 two bacteriohopanoids with acyclic pentol side-chains from the cyanobacterium *Nostoc*
697 PCC 6720. Tetrahedron. 52:2777-2788. 10.1016/j.orggeochem.2014.02.004
698 42. Ricci JN, Morton R, Kulkarni G, Summers ML, Newman DK. 2016. Hopanoids play a
699 role in stress tolerance and nutrient storage in the cyanobacterium *Nostoc punctiforme*.
700 Geobiology. 15:173-183. 10.1111/gbi.12204
701 43. Ricci JN, Coleman ML, Welander PV, Sessions AL, Summons RE, Spear JR, Newman
702 DK. 2013. Diverse capacity for 2-methylhopanoid production correlates with a specific
703 ecological niche. The ISME Journal. 8:675-684. 10.1038/ismej.2013.191
704 44. Sepúlveda J, Wendler J, Leider A, Kuss H-J, Summons RE, Hinrichs K-U. 2009.
705 Molecular isotopic evidence of environmental and ecological changes across the
706 Cenomanian–Turonian boundary in the Levant Platform of central Jordan. Organic
707 Geochemistry. 40:553-568. 10.1016/j.orggeochem.2009.02.009
708 45. Sepúlveda J, Wendler JE, Summons RE, Hinrichs K-U. 2009. Rapid resurgence of marine
709 productivity after the Cretaceous-Paleogene mass extinction. Science. 326:129-132.
710 10.1126/science.1176233
711 46. French KL, Tosca NJ, Cao C, Summons RE. 2012. Diagenetic and detrital origin of
712 moretane anomalies through the Permian–Triassic boundary. Geochim Cosmochim Acta.
713 84:104-125. 10.1016/j.gca.2012.01.004
714 47. Campbell EL, Summers ML, Christman H, Martin ME, Meeks JC. 2007. Global gene
715 expression patterns of *Nostoc punctiforme* in steady-state dinitrogen-grown heterocyst-
716 containing cultures and at single time points during the differentiation of akinetes and
717 hormogonia. Journal of Bacteriology. 189:5247-5256. 10.1128/JB.00360-07

48. Cohen MF, Meeks JC. 1997. A hormogonium regulating locus, hrmUA, of the cyanobacterium *Nostoc punctiforme* strain ATCC 29133 and its response to an extract of a symbiotic plant partner *Anthoceros punctatus*. Molecular Plant-Microbe Interactions. 10:280-289. 10.1094/MPMI.1997.10.2.280
49. Cai YP, Wolk CP. 1990. Use of a conditionally lethal gene in *Anabaena* sp. strain PCC 7120 to select for double recombinants and to entrap insertion sequences. Journal of Bacteriology. 172:3138-3145. 10.1128/jb.172.6.3138-3145.1990
50. Meeks JC, Castenholz RW. 1971. Growth and photosynthesis in an extreme thermophile, *Synechococcus lividus* (Cyanophyta). Arch Mikrobiol. 78:25-41. 10.1007/BF00409086
51. Cohen MF, Wallis JG, Campbell EL, Meeks JC. 1994. Transposon mutagenesis of Nostoc sp. strain ATCC 29133, a filamentous cyanobacterium with multiple cellular differentiation alternatives. Microbiology 140:3233-3240. 10.1099/13500872-140-12-3233
52. Talbot HM, Watson DF, Murrell JC, Carter JF, Farrimond P. 2001. Analysis of intact bacteriohopanepolyols from methanotrophic bacteria by reversed-phase high-performance liquid chromatography-atmospheric pressure chemical ionisation mass spectrometry. Journal of chromatography A. 921:175-185. 10.1016/S0021-9673(01)00871-8
53. Talbot HM, Rohmer M, Farrimond P. 2007. Rapid structural elucidation of composite bacterial hopanoids by atmospheric pressure chemical ionisation liquid chromatography/ion trap mass spectrometry. Rapid Commun Mass Spectrom. 21:880-892. 10.1002/rcm.2911
54. Talbot HM, Summons R, Jahnke L, Farrimond P. 2003. Characteristic fragmentation of bacteriohopanepolyols during atmospheric pressure chemical ionisation liquid chromatography/ion trap mass spectrometry. Rapid Commun Mass Spectrom. 17:2788-2796. 10.1002/rcm.1265
55. Welander PV, Doughty DM, Wu CH, Mehay S, Summons RE, Newman DK. 2012. Identification and characterization of *Rhodopseudomonas palustris* TIE-1 hopanoid biosynthesis mutants. Geobiology. 10:163-177. 10.1111/j.1472-4669.2011.00314.x
56. Wong FCY, Meeks JC. 2002. Establishment of a functional symbiosis between the cyanobacterium *Nostoc punctiforme* and the bryophyte *Anthoceros punctatus* requires genes involved in nitrogen control and initiation of heterocyst differentiation. Microbiology. 148:315-323. 10.1099/00221287-148-1-315
57. Olsson-Francis K, de la Torre R, Towner MC, Cockell CS. 2009. Survival of akinetes (resting-state cells of cyanobacteria) in low earth orbit and simulated extraterrestrial conditions. Origins of life and evolution of the biosphere : the journal of the International Society for the Study of the Origin of Life. 39:565-579. 10.1007/s11084-009-9167-4
58. Yamamoto Y. 1975. Effect of desiccation on the germination of akinetes of *Anabaena cylindrica*. Plant and Cell Physiology. 16:749-752. 10.1093/oxfordjournals.pcp.a075195
59. Jungblut AD, Allen MA, Burns BP, Neilan BA. 2009. Lipid biomarker analysis of cyanobacteria-dominated microbial mats in meltwater ponds on the McMurdo Ice Shelf, Antarctica. Organic Geochemistry. 40:258-269. 10.1016/j.orggeochem.2008.10.002
60. Rethemeyer J, Schubotz F, Talbot HM, Cooke MP, Hinrichs K-U, Mollenhauer G. 2010. Distribution of polar membrane lipids in permafrost soils and sediments of a small high Arctic catchment Organic Geochemistry. 41:1130-1145. 10.1016/j.orggeochem.2010.06.004
61. Schmerk CL, Bernards MA, Valvano MA. 2011. Hopanoid production is required for low-pH tolerance, antimicrobial resistance, and motility in *Burkholderia cenocepacia*. Journal of Bacteriology. 193:6712-6723. 10.1128/JB.05979-11
62. Rajeev L, da Rocha UN, Klitgord N, Luning EG, Fortney J, Axen SD, Shih PM, Bouskill NJ, Bowen BP, Kerfeld CA, Garcia-Pichel F, Brodie EL, Northen TR, Mukhopadhyay A.

2013. Dynamic cyanobacterial response to hydration and dehydration in a desert biological soil crust. ISME J. 7:2178-2191. 10.1038/ismej.2013.83

771

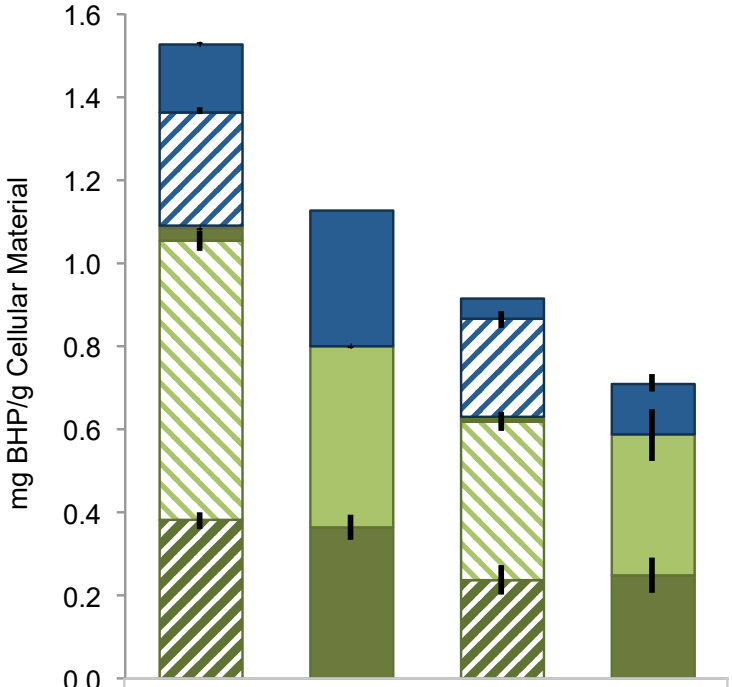

	WT Veg. Cells	Δ*hpnP* Veg. Cells	WT Akinetes	Δ*hpnP* Akinetes
BHT	0.163	0.330	0.052	0.124
2-MeBHT	0.272	0.000	0.236	0.000
BHpentol-1	0.011	0.434	0.003	0.338
BHpentol-2	0.027	0.363	0.006	0.249
2-MeBHpentol-1	0.675	0.000	0.382	0.000
2-MeBHpentol-2	0.379	0.000	0.237	0.000

772

773 **Figure 1.**

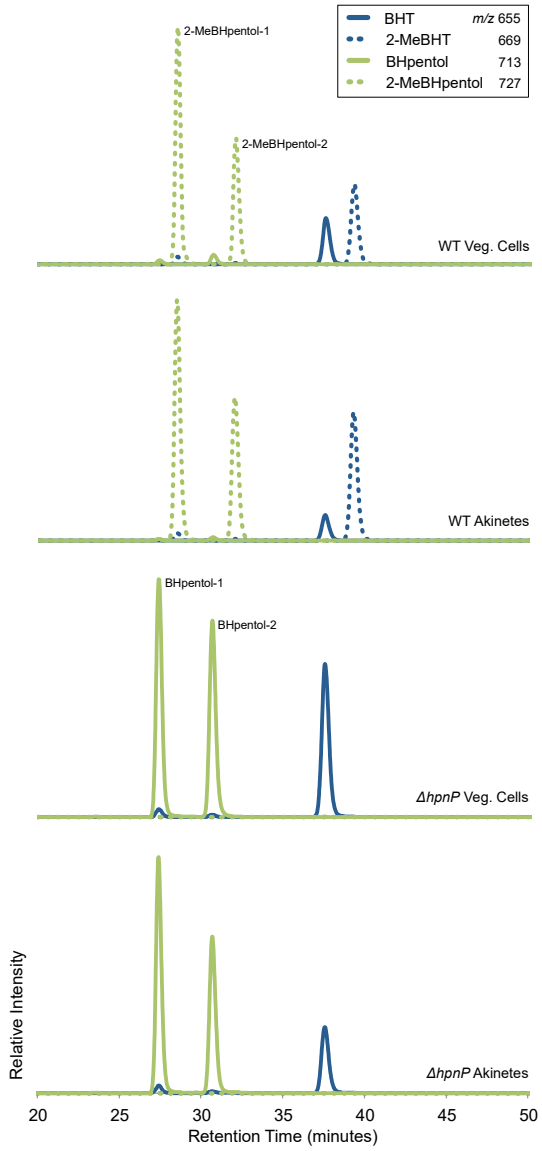

774

775 **Figure 2.**

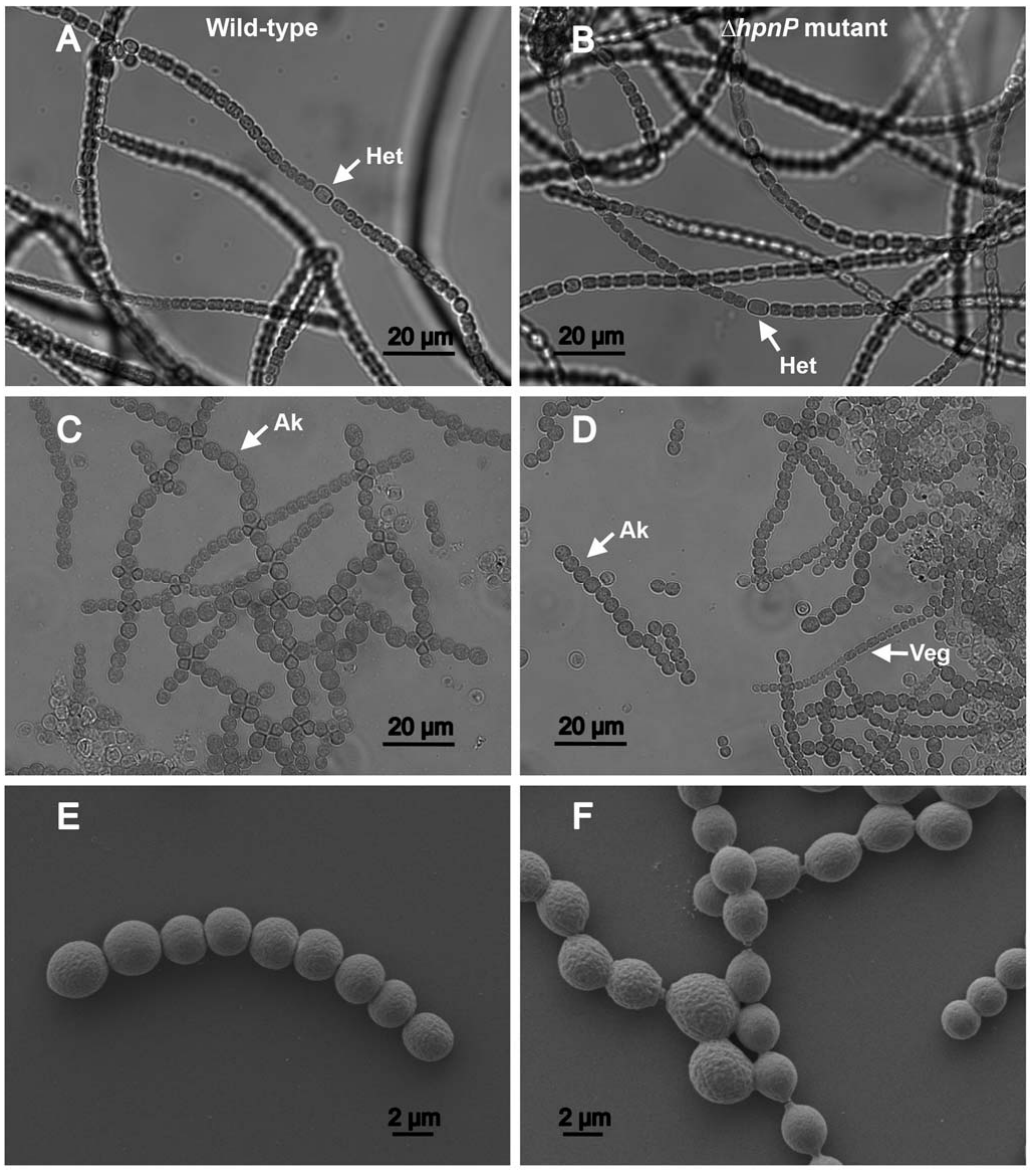

776

777 **Figure 3.**

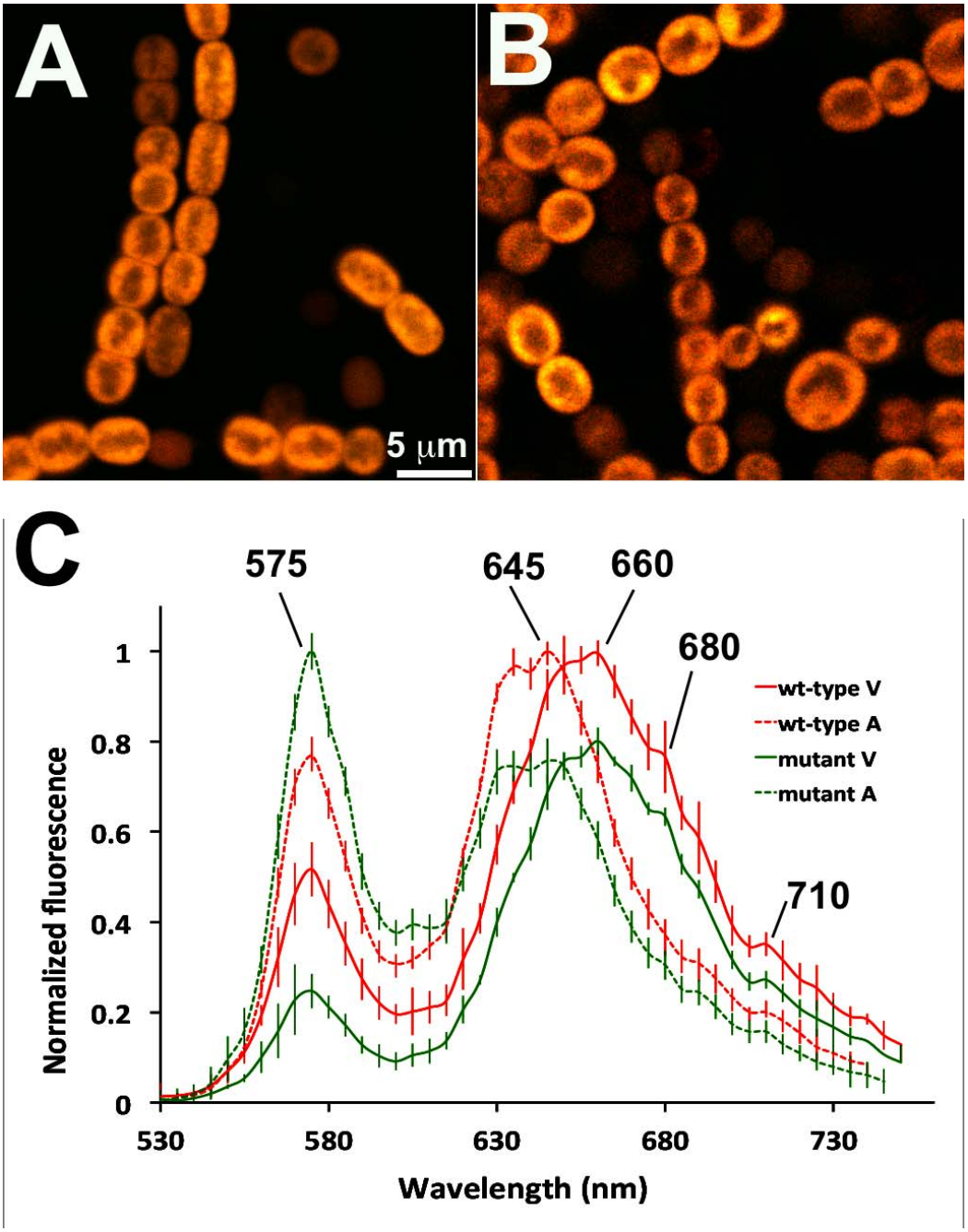

778

779 **Figure 4.**

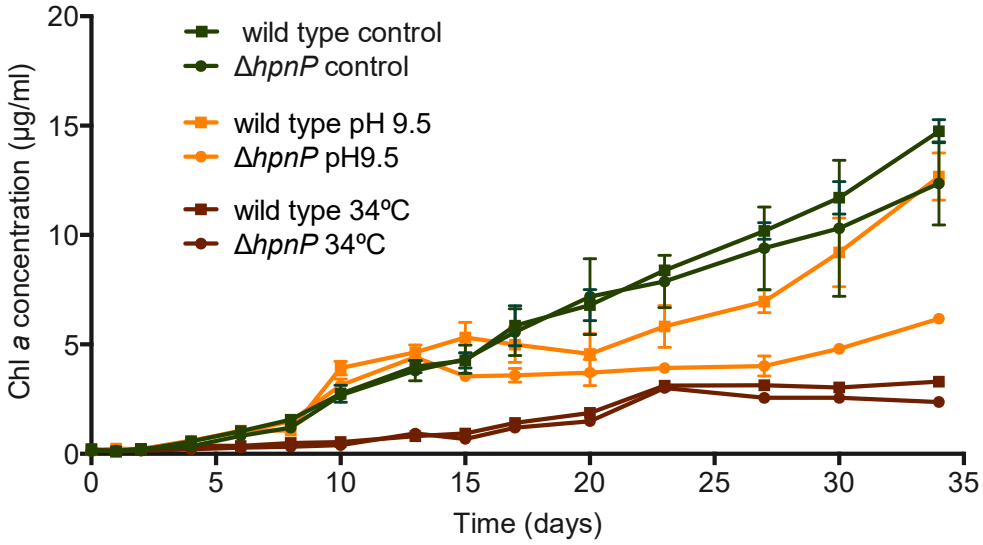

780

781 **Figure 5.**

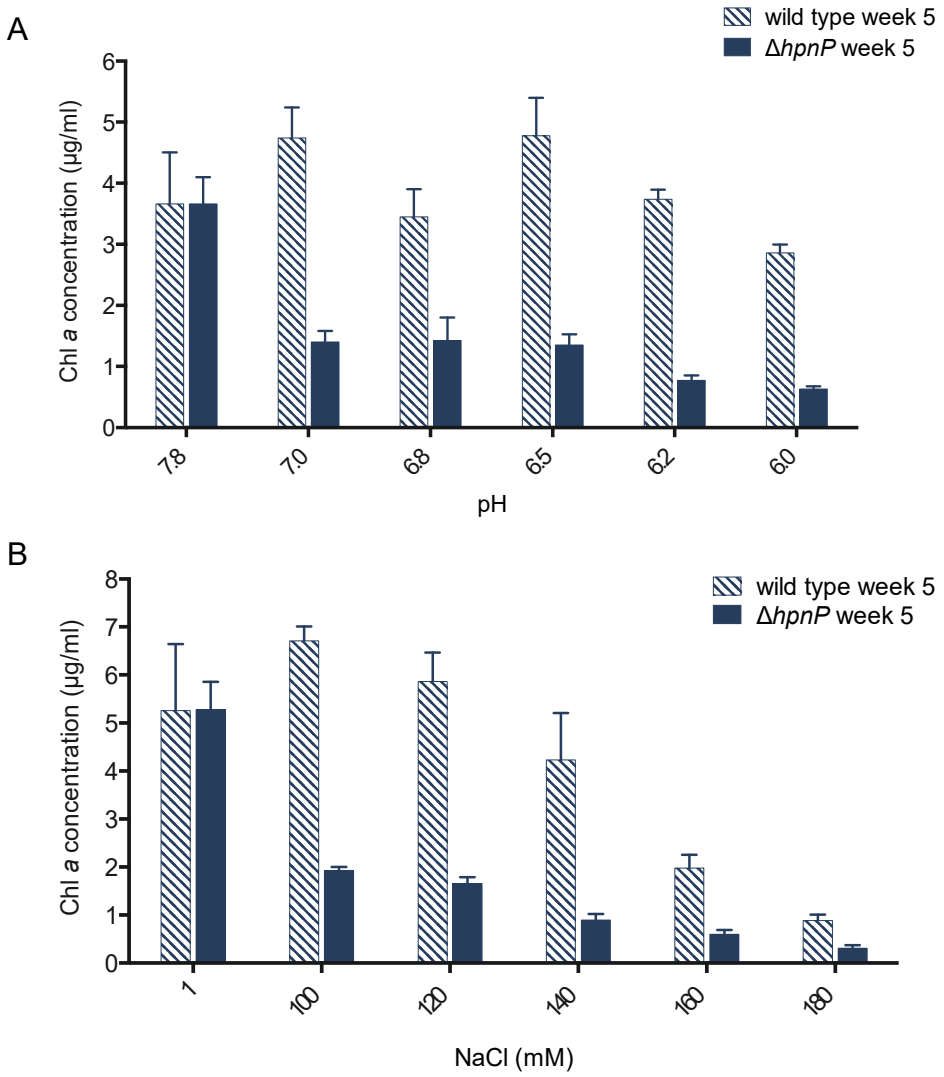

782

783 **Figure 6.**